JOURNAL OF MATERIALS SCIENCE 9 (1974) 349–358

Hardness anisotropy in niobium carbide

G. MORGAN, M. H. LEWIS
Department of Physics, University of Warwick, Coventry, Warwickshire, UK

Measurements of hardness anisotropy by Knoop diamond indentation on the {100} surfaces of Nb_6C_5 crystals show that the hardness is determined by crystallographic slip on {111} ⟨1$\bar{1}$0⟩ and {110} ⟨1$\bar{1}$0⟩ systems. {111} is the preferred slip plane for Nb_6C_5 and crystals with higher carbon content which show a marked decrease in Knoop hardness. The carbon atom/vacancy arrangement in these crystals is shown, by electron diffraction, to possess short-range order. Crystals annealed at low temperatures contain domains of non-cubic long-range order which increase the Knoop hardness and eliminate the anisotropy in hardness. Dislocation arrangements around Knoop indentations have been directly observed by electron microscopy in an attempt to confirm the slip processes deduced from hardness anisotropy.

1. Introduction

The nominally cubic (NaCl type) carbides of the group IV and V transition elements exhibit macroscopic plasticity under uniaxial stress above 0.4 to 0.5 T_m (where T_m is the absolute melting point). The plasticity results from dislocation motion on {111} ⟨1$\bar{1}$0⟩ slip systems, similar to fcc metals, and results in a measurable polycrystalline ductility, associated with five independent slip systems. The extreme temperature sensitivity of the single crystal flow-stress below 0.4 T_m results in a normally brittle behaviour under conditions of uniaxial stress. However, some insight into plastic deformation mechanisms in these materials at low temperatures may be obtained by imposing a hydrostatic stress component. This is most conveniently achieved by a simple indentation hardness test. The Knoop indentation test, using an elongated diamond indenter, has been extensively used to determine the relative hardness of intrinsically "hard" and brittle materials but has a particular advantage in detecting anisotropy in the hardness of single crystals. The measured hardness anisotropy has been used as indirect evidence for crystallographic slip processes which control the hardness value and, by comparison with simple theory [1], may be used to estimate the flow-stress ratios for different slip systems.

Knoop indentation experiments on single crystals of groups IV and V transition metal carbides [2, 3] indicate that {110} ⟨1$\bar{1}$0⟩ is an important slip system in addition to {111} ⟨1$\bar{1}$0⟩ and for certain compounds and deviations from stoichiometric composition is the preferred system at room temperature. Thus, for the group IV compounds $TiC_{0.8}$ and $HfC_{0.98}$, the flow stress for the {110} ⟨1$\bar{1}$0⟩ system is smaller than for {111} ⟨1$\bar{1}$0⟩. Comparison of hardness values for $TiC_{0.8}$ and $TiC_{0.97}$ indicate a softening with increasing deviation from stoichiometric composition [4]. This behaviour is in marked contrast to that for the group V compound TaC which increases rapidly in hardness from $TaC_{0.96}$ to $TaC_{0.83}$ [5] and which changes its slip plane preference from {111} to {110} with decreasing carbon content [3]. These results have been explained [3] in terms of the differences in degree of close-packing of the metal atom substructure between group IV and V compounds and with varying composition. Thus, an increasing degree of non-stoichiometry for group V compounds promotes closer packing of metal atoms which results in increased hardness and a preference for {110} ⟨110⟩ slip normally observed for the closer packed group IV compounds. The group V compound $VC_{0.84}$ exhibits high hardness and a preference for {110} ⟨1$\bar{1}$0⟩ slip [3] and is, therefore, comparable with the group IV or non-stoichiometric group V behaviour. However, it is considered to be slightly anomalous in being near to the upper limit of composition ($VC_{0.98}$) and the inability to suppress the formation of a number of long-range ordered phases at low temperatures, based on different arrangements of carbon atoms and vacancies

arising from the non-stoichiometry [6-9]. This behaviour contrasts that of TaC in which the non-stoichiometric vacancies do not form long-range ordered arrangements [10].

This paper is concerned with hardness anisotropy in the group V compound NbC which offers a particular advantage in the possibility of studying slip geometry in crystals with or without long-range ordered vacancy arrangements for the same composition [8].

A recent comparison of hardness anisotropy at different temperatures for a number of transition metal carbides includes a result for a crystal of composition $NbC_{0.87}$ at 25°C [11]. However, the state of carbon atom order in this crystal was not precisely known and the compositions and heat-treatments required to form long-range order have subsequently been determined [8].

The main aims of the research described here were (1) to obtain information about low temperature deformation mechanisms in niobium carbide via measurements of hardness anisotropy, (2) to determine how the anisotropy and absolute hardness vary with the degree of non-stoichiometry and with carbon atom ordering, and (3) to correlate hardness anisotropy with direct observations of dislocations in the indented crystal.

2. Experimental techniques

2.1. Hardness measurements

A single crystal of approximate composition $NbC_{0.83}$ (Nb_6C_5) was spark-cut into 0.5 mm slices, parallel to {100}, following orientation analysis by the Laue X-ray technique. The slices were mechanically polished through various grades of silicon carbide paper and finally with successively finer grades of diamond paste to obtain a mirror surface for micro-indentation. The slices were mounted on metal discs and the ⟨100⟩ NbC directions inscribed on the discs after a further X-ray orientation analysis.

Micro-indentations were made on the {100} surfaces using loads of 100, 150 and 200 g with the long axis of the Knoop diamond (contained in a modified McCrone microhardness apparatus, mounted on an inverted optical microscope) at various angles from the ⟨100⟩ NbC directions. The most consistent absolute hardness values were obtained from the series at 150 g load but a similar anisotropy factor was obtained for all loads used. A minimum of ten indents were made for each indenter orientation and applied load and the loading cycle standardized with a period of 15 sec at full load.

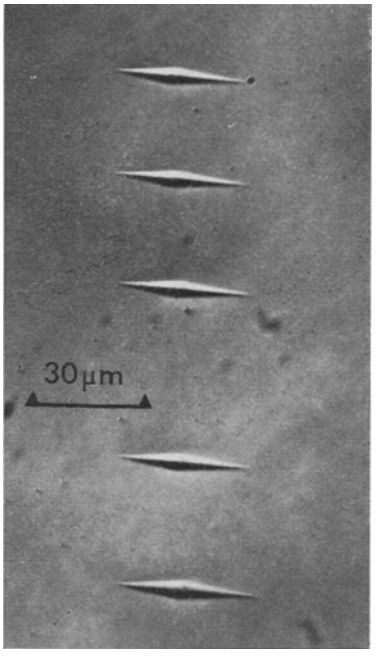

Figure 1 Knoop indentations on the {100} polished surface of a Nb_6C_5 crystal viewed under oblique illumination.

The indentation lengths were measured on a Zeiss Ultraphot microscope, using oblique illumination (Fig. 1), a micrometer eyepiece and movable cross-wires. Knoop hardness values (H_K) were calculated using the empirical formula

$$H_K = \frac{14230\,P}{L^2}\ \text{kg mm}^{-2}$$

where P is the indenting load (g) and L is the length of indent (μm).

Hardness anisotropy was determined on single crystal slices, (1) in the "as-grown" state, (2) on specimens annealed to produce long range ordered carbon atom/vacancy arrangements, and (3) on specimens which had been carburized by diffusion of carbon from an "aquadag" surface coating at 1000°C.

2.2. Microstructural observations

The micro-topography of the indented surfaces was examined by optical-interference microscopy and scanning electron microscopy. Attempts were made to reveal dislocation distributions

around indentations by surface etch-pitting. An aqueous solution of 20% potassium ferricyanide and 20% potassium hydroxide was successful in revealing dislocation sub-grain boundaries but did not produce discrete pits around indentations.

Dislocation arrangements in the localized deformed volume of crystal adjacent to indentations were examined by transmission electron microscopy of thin crystals prepared by the following sequence. Discs, 3 mm diameter, were cut from the polished crystal slices and multiply indented at a constant angle (0° or 45° from ⟨100⟩). The discs were mounted in a conventional PTFE holder and electropolished to perforation using a 5% solution of sulphuric acid in methanol. During electropolishing, the indented surface was preserved by a "Lacomit" coating. A necessary final step was that of ion-beam machining on both surfaces (using 5 keV argon ions for 1 to 3 h) to remove the thin mechanically polished surface layer and to markedly increase the area of electron transparency adjacent to the indentations. The 3 mm discs prepared in this way were mounted in the goniometer specimen holder of a JEM 200 electron microscope. Similar disc-shaped specimens which had not been indented, but given a simple electro-thinning treatment were used in analysis of the state of carbon atom order by electron diffraction and microscopy.

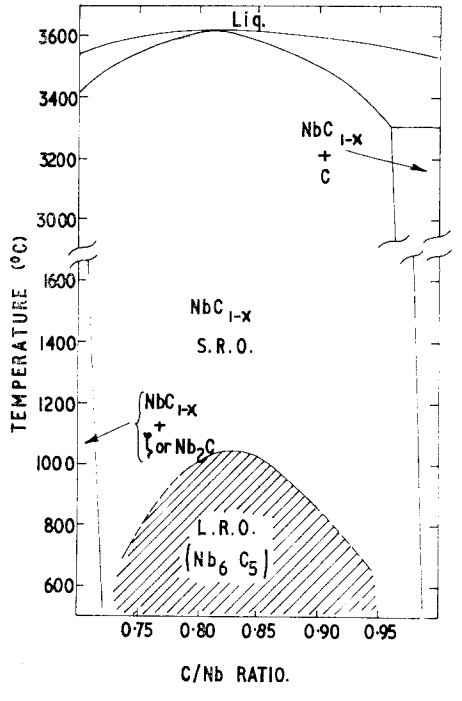

Figure 2 Part of a phase diagram for the Nb-C system showing approximate limits of formation of the long-range ordered phase based on the composition Nb_6C_5 (from Billingham *et al* [12]).

3. Carbon atom/vacancy distributions

The partial phase diagram for the Nb-C system (Fig. 2) has been constructed from a previous electron diffraction study of compounds within the nominally cubic (NaCl structure type) phase field [8]. The low temperature shaded region of the NbC_{1-x} phase field is that in which a long-range ordered (LRO) carbon atom/vacancy arrangement is developed after long annealing treatments. In crystals which have been rapidly cooled from above the shaded region, the carbon atom/vacancy arrangement is not completely random and results in electron diffraction patterns of the type shown in Fig. 3a, from a crystal

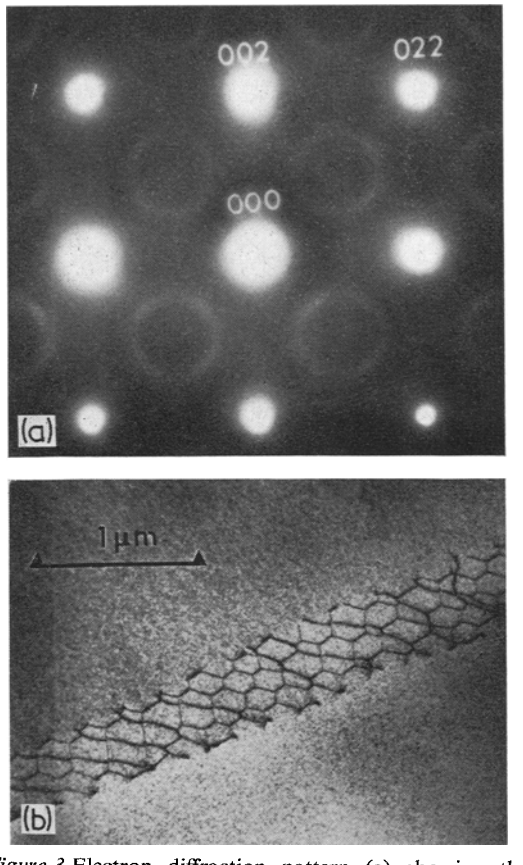

Figure 3 Electron diffraction pattern (a) showing the diffuse bands of intensity indicative of a short-range ordered carbon atom arrangement in a crystal of Nb_6C_5. Electron microscope images are featureless apart from sparsely distributed grown-in dislocation boundaries (b).

in the "as-grown" state used for some of the hardness anisotropy experiments. This "short-range" ordered (SRO) state is found in many sub-stoichiometric carbides and nitrides of transition metals and has been analysed [12, 13] in terms of the most probable metal atom/interstitial atom co-ordination and which resembles that which has been determined exactly for the long-range ordered state in vanadium and niobium carbides [8, 9].

From the viewpoint of microhardness anisotropy the most important distinction between the two states (SRO and LRO) lies in the anisotropic crystal distortion accompanying the long-range ordered state. A detailed description of the long-range ordered structure has been given elsewhere [9] and only the more important features of structure relevant to dislocation motion will be outlined here. Long-range order is detected by the presence of sharp superlattice diffraction spots (Fig. 4a) which have been used to define a carbon atom sublattice with monoclinic symmetry [9]. The non-stoichiometric vacancies are uniformally arranged within layers parallel to {111} cubic parent lattice planes. The layer plane is parallel to (010) monoclinic and is defined by an alternating complete/incomplete sequence in the filling of octahedrally co-ordinated sites forming carbon atom planes parallel to a particular choice of {111} cubic plane (Fig. 4c). "Domains" corresponding to a particular choice of {111} layer plane are most conveniently imaged in dark field using a superlattice reflection (Fig. 4b). Substructure, visible within domains (Fig. 4b), is composed of the three possible variants of monoclinic unit cell axes within the "layer" plane and a faulting in the vacancy-containing layer stacking sequence [8, 9]. A distortion of the fcc vanadium atom substructure accompanies the reduction in symmetry of the carbon atom substructure and is mainly that of contraction normal to the "layer" plane in each domain. Thus adjacent

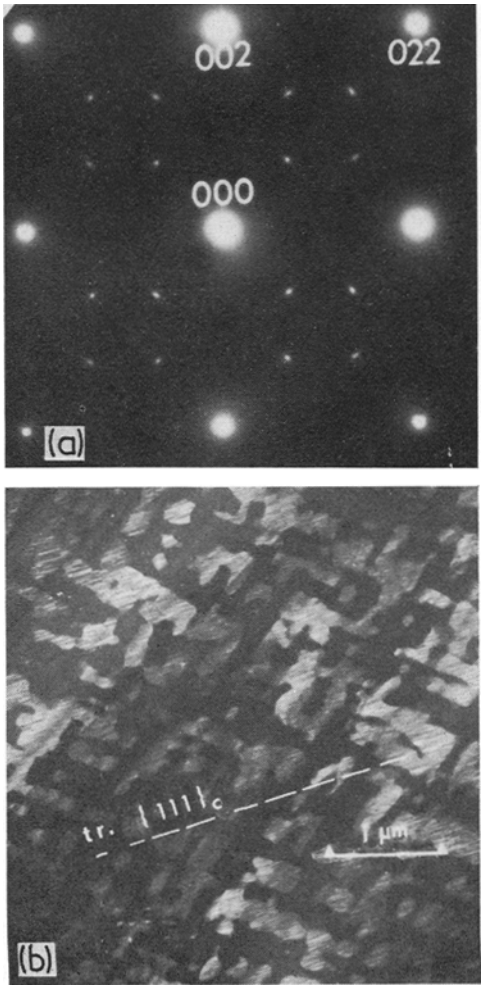

Figure 4 Electron diffraction pattern (a) from a long-range ordered Nb_6C_5 crystal in ⟨100⟩ orientation for comparison with Fig. 3a. The dark-field image (b) has been recorded with a monoclinic superlattice reflection from a crystal in ⟨112⟩ parent lattice orientation. The "domains" visible in (b) correspond to one of four possible variants of (010) monoclinic layer plane orientation (c).

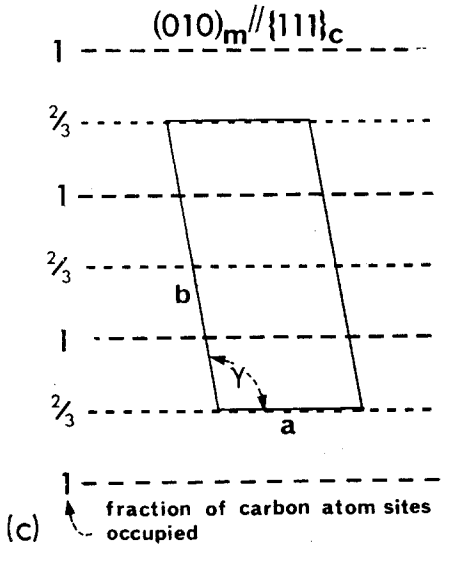

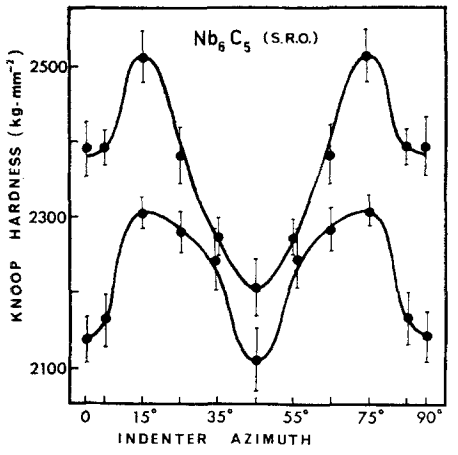

Figure 5 Variation of Knoop hardness on a (001) surface with indenter angle (from [100]). The two curves are for different single crystal discs of Nb_6C_5 in the short-range ordered state and an indenter load of 150 g.

domains are associated with different ⟨111⟩ distortions.

4. Hardness anisotropy

4.1. Observations

Two independent series of indentations at 150 g load were recorded for crystals of a given composition or structural state. The Knoop hardness values with varying indenter orientation are shown for "as-grown" crystals of $NbC_{0.83}$ in the SRO state (Fig. 5), carburized crystals in the SRO state (Fig. 6) and annealed crystals of $NbC_{0.83}$ in the LRO state (Fig. 6).

The graphical values have been obtained by taking the mean of twenty readings (ten from each mirror symmetry position on either side of ⟨110⟩, e.g. 0° and 90°, 15° and 75° etc.). In this way systematic errors arising from deviations of the polished surface from {100} or indenter rotation axis not being normal to the polished surface are minimized. Thus the graphs have been drawn with mirror symmetry about the 45° position on the abscissa, consistent with the cubic crystal symmetry. The error bars shown on the graphs are the mean values of the standard error in hardness value for the symmetrically equivalent indenter orientations.

The most striking observation is the difference in Knoop hardness anisotropy between Figs. 5 and 6 with significant variations in absolute hardness value. Crystals in the "as-grown" state, of composition near to Nb_6C_5, show an increase

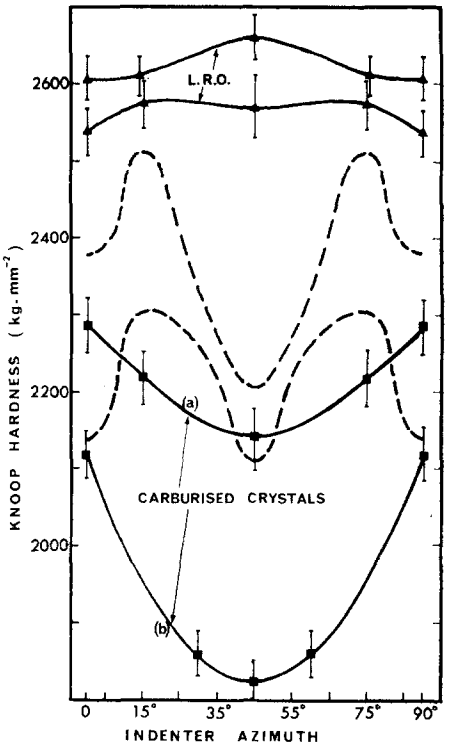

Figure 6 Variation of Knoop hardness with indenter angle on a (001) surface for Nb_6C_5 crystals in (1) the long-range ordered state and (2) the short-range ordered state which have been carburized such that (b) is of higher carbon content than (a). The curves from Fig. 5 are shown with broken lines for comparison.

in H_K from 0° to 15°, decreasing to a minimum at 45° which has a lower value than at 0°.

The occurrence of a hardness maximum between 0° and 45° is consistent with the result obtained by Hannink *et al* [11] except that their 45° hardness value is slightly lower than at the 0° orientation.

"Carburized" crystals exhibit a continuous decrease in H_K from 0° to 45°. There is a decrease in H_K with increase in carbon content for all indenter orientations. The curves (a) and (b) in Fig. 6 were obtained from slightly different depths below the carburized crystal surface. The crystal of Nb_6C_5 in the long range ordered state shows a significant increase in average H_K with a marked loss in hardness anisotropy from the short-range ordered state. These observations will be discussed in relation to existing theory for hardness anisotropy.

4.2. Discussion

4.2.1. "As-grown" crystals

The anisotropy in microhardness observed for niobium carbide and previously for other transition metal carbides [2, 3, 11] indicates that it is an intrinsic property of the crystal and may be related to the distribution of shear stresses produced in the crystal adjacent to the Knoop indenter. Confirmation of a dislocation mechanism for crystal plasticity adjacent to the indenter has been obtained previously by etch-pitting [2, 5] and in the present work by direct electron microscope imaging, discussed below. A recent analysis of hardness anisotropy on different crystallographic surfaces and for different preferred slip systems [1] is based on the earlier explanations of Daniels and Dunn [14] who considered the constraints to deformation of small volumes of crystal adjacent to the indenter facets. Thus a crystal would appear to be least hard (i.e. produce a larger indentation for a given load) when the indenter orientation was such that (1) it resulted in the greatest resolved shear stress on the preferred slip system and (2) allowed rotation of the crystal such as to displace material to the crystal surface (from the bulk position finally occupied by the indenter). The second factor means that a slip system which allows rotation of slip planes about an axis parallel to the indenter facets will be favoured. Hence, the maximum constraint to slip plane rotation occurs when the angle ψ between rotation axis and indenter facet = 90°. The "effective resolved shear stress" (τ_e) equation developed by Daniels and Dunn includes cos ψ in addition to the usual angles associated with the Schmid factor. Thus $\tau_e = \sigma \cos\lambda \cos\phi \cos\psi$, where σ is the applied axial stress (on a cylindrical element of crystal with its axis parallel to the steepest slope of an adjacent indenter facet) whose absolute value may not be determined for the Knoop test but is unimportant since the product of cosines is the important factor when considering hardness anisotropy.

Brookes *et al* [1] have modified the Daniels and Dunn equation with an additional rotational constraint term involving the angle γ between slip direction and adjacent facet. The final equation is written:

$$\tau_e' = \sigma \cos\lambda \cos\phi \tfrac{1}{2}(\cos\psi + \sin\gamma) .$$

Families of curves representing the mean value of τ_e' (for four Knoop indenter facets) have been produced for different crystal surfaces and indenter orientations. The approximate validity of this equation has been demonstrated for a range of materials with well-established slip systems.

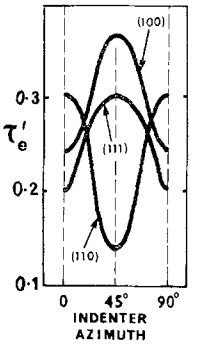

Figure 7 Calculated values of "effective resolved shear stress", τ_e', for {111} ⟨1$\bar{1}$0⟩, {110} ⟨1$\bar{1}$0⟩ and {001} ⟨1$\bar{1}$0⟩ slip systems with varying indenter orientation on the {100} surface of a cubic crystal (after Brookes *et al* [1]).

The form of τ_e' with varying indenter orientation on a cubic {100} surface is reproduced in Fig. 7 for primary slip systems {111} ⟨1$\bar{1}$0⟩, {001} ⟨1$\bar{1}$0⟩ and {110} ⟨1$\bar{1}$0⟩. A comparison of these curves with the experimentally observed hardness anisotropy on the "as-grown" $NbC_{0.88}$ {100} surfaces shows that its preferred slip systems are {111} ⟨1$\bar{1}$0⟩. Slip occurs predominantly on this system until the indenter orientation is smaller than 15 to 20° from ⟨100⟩ where the fall in hardness indicates major operation of the {110} ⟨1$\bar{1}$0⟩ systems which are subject to a much higher effective resolved shear stress (τ_e', Fig. 7). The fact that the "cross-over" in τ_e' occurs at about 22° indicates that the critical resolved shear stress (τ_c) for slip is smaller on the {111} ⟨1$\bar{1}$0⟩ system. The occurrence of a hardness maximum between 0° and 45° may also be interpreted as a change in primary slip system from {110} ⟨1$\bar{1}$0⟩ to {001} ⟨1$\bar{1}$0⟩ since the curve for τ_e' for the latter system shows a maximum at the 45° orientation (Fig. 7). In view of {111} ⟨1$\bar{1}$0⟩ being the preferred slip system for group IV and V carbides at elevated temperature [15], the alternative explanation of {001} ⟨110⟩ slip is unlikely.

4.2.2. Effect of composition

The absence of an intermediate hardness maximum between 0° and 45° in the carburized

sections (Fig. 6) indicates that, for all indenter orientations, slip occurs predominantly on the system $\{111\}\langle 1\bar{1}0\rangle$. Thus, the ratio of flow stresses on $\{111\}$ and $\{110\}$ planes must decrease with increasing carbon content above Nb_6C_5. This is associated with a decrease in the absolute value of flow stress on $\{111\}$ planes, indicated by comparison of hardness values at 45° orientation for the different compositions.

Similar effects of composition on hardness anisotropy occur in tantalum carbide. Rowcliffe and Hollox [2] report a continuous decrease in Knoop hardness from 0° to 45° for a composition $TaC_{0.96}$, indicating $\{111\}$ preferred slip. However, for a "decarburized" crystal, $TaC_{<0.96}$, the ratio of flow stresses on $\{111\}$ and $\{110\}$ planes exceeds one, indicated by a higher hardness value at 45° than at 0° [3]. Thus, unlike tantalum carbide, a small preference for $\{111\}$ slip in niobium carbide is maintained down to the substoichiometric Nb_6C_5. The increase in hardness with decreasing carbon content has also been observed for tantalum carbide [3, 5] for compositions between $TaC_{0.96}$ and $TaC_{0.83}$ (Ta_6C_5). An explanation of this composition dependence has been attempted by Rowcliffe and Hollox [3] using a hard sphere model which distinguishes between the nearly stoichiometric carbides of groups IV and V. A comparison of lattice parameters for parent metal and carbide suggests that group IV carbides are more ideally close packed, with radius ratios approaching the value 0.414 for octahedral co-ordination, whereas group V carbides are more open structures, having larger radius ratios. Hence, it is argued [3] that the greater low temperature ductility and preferred $\{111\}\langle 1\bar{1}0\rangle$ slip of nearly stoichiometric group V carbides arises from easier dissociation of dislocations on this system for the more open structure. With decreasing carbon content a decrease in lattice parameter indicates a tendency to the more close-packed group IV behaviour in which the flow stresses on $\{111\}$ and $\{110\}$ are similar and in most compounds $\{110\}$ is preferred.

This model is incomplete since it does not explain the hardness maximum observed at $TaC_{0.83}$ [5]. It is significant that this composition lies close to that of the melting point maxima for group V carbides and to the maximum in critical temperature for transformation to long range order in vanadium and niobium carbides [8, 12]. A qualitative description of atomic bonding in carbides which is able to explain the ordering and melting point maxima has been given by Lye [16] and may be used as a more general model for the hardness-composition relation. According to this model, electrons derived from carbon 2p states are redistributed into normally vacant states in lower lying d bands, associated with metal atoms, thus increasing the occupancy of d states whose orbitals overlap in a bonding configuration. Lye has suggested that for vanadium carbide these states (associated with bonding orbitals) are completely filled for a carbon atom concentration equivalent to V_6C_5, above which antibonding states are increasingly occupied. A maximum in the cohesive energy and crystal melting point is, therefore, expected to occur at this composition and the crystal will prefer an ordered carbon atom distribution with five-fold co-ordination of all vanadium atoms [10]. This condition is found at low temperatures in both vanadium and niobium carbides and is also the preferred co-ordination identified in the short-range ordered state in tantalum carbide [10] and at elevated temperatures in the vanadium and niobium carbides [12, 13]. A reduction in driving force for ordering in the series from V → Nb → Ta carbides (indicated by a reduction in critical temperature for long-range order) may be explained [10] by the increase in carbon content, above M_6C_5, at which the bonding states are fully occupied. However, the composition Nb_6C_5 is near to the maximum in critical temperature for long-range order in this compound [12].

By correlating a maximum in cohesive energy of the crystal with a maximum in the Peierls stress for dislocation motion an intermediate hardness maximum with deviation from stoichiometry is adequately explained. Compositional deviations from M_6C_5 reduce the homogeneity of the structure and, therefore, the bond strength in both long- and short-range ordered states. If the degree of short-range order decreases rapidly above the critical temperature, the extreme temperature dependence of Peierls stress for these compounds may also be explained.

Preliminary measurements on decarburized Nb_6C_5 crystals indicate a reduction in Knoop hardness similar to decarburized tantalum carbide but the composition of the hardness maximum has not been precisely determined. A similar comparison for vanadium carbide is not possible in view of the inability to retain the short-range ordered state throughout the composition range.

4.2.3. Ordered crystals

The higher value and loss of anisotropy in Knoop hardness for long-range ordered crystals may be explained with reference to Fig. 4. The non-cubic symmetry in carbon atom arrangement and associated niobium sublattice distortion is expected to result in differences in flow stress for different {1 1 1} cubic parent lattice planes. Hence, each "domain" (Fig. 4) is expected to have a singular plane (the (0 1 0) monoclinic "layer" plane) on which dislocation motion is preferred. The assembly of domains in different orientations will, therefore, approach the isotropic hardness behaviour of polycrystalline material if the indenter size is much greater than that of a single domain.

An increased mean hardness value is expected to originate from the superposition of various mechanisms; (1) a domain boundary hardening mechanism, owing to non-coincidence of preferred (0 1 0) monoclinic slip plane in adjacent domains, (2) an increase in the Peierls stress for dislocation motion in a crystal which has a higher cohesive energy resulting from the preferred ordered state. A boundary hardening mechanism similar to (1) has been suggested by Hannink and Murray [17] for ordered $VC_{0.84}$ which shows a domain size dependence of Vickers hardness. A Knoop hardness test on a $VC_{0.84}$ crystal (in which the ordering reaction cannot be suppressed) by Rowcliffe and Hollox [3] surprisingly shows a pronounced anisotropy but in this compound, domains are usually much larger than for Nb_6C_5 (Fig. 4) and may be comparable with the indented volume for the 100 g load used in these tests [3]. A further unknown factor is the density of planar imperfection substructure within domains of V_6C_5 which varies with prior heat-treatment [8, 9]. This is expected to influence the ratio of flow stresses between (0 1 0) monoclinic slip planes and other (previously {1 1 1} cubic) planes within the ordered domains.

5. Indentation microstructure

Observations of Knoop hardness anisotropy indicate that the mechanism controlling the anisotropy is that of dislocation motion on preferred slip planes in the small volume of material adjacent to the indenter. As the crystallinity of the material beneath the indenter is maintained, the process must involve a displacement from the bulk to a position above that of the original plane surface. The displacement

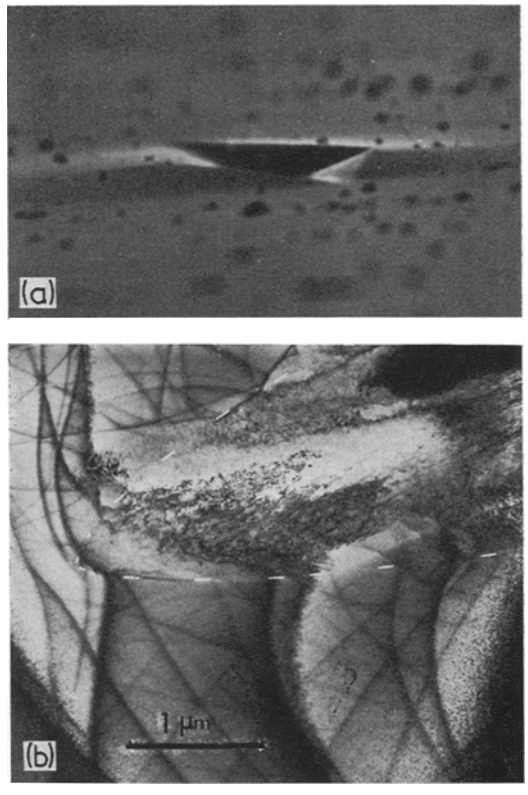

Figure 8 Scanning electron micrograph (a) showing the crystal surface displacement surrounding a Knoop indentation viewed in a direction near to its long axis. The transmission electron micrograph (b) shows that lattice rotations (indicated by discontinuity in extinction contours) occur within the small volume of deformation round the indentation.

is believed to occur mainly by a crystal rotation and this is the origin of the "rotational constraint" term in the equations for τ_e' [1, 13]. For intrinsically hard materials, such as niobium carbide, the deformed volume is localized, near to the indenter facets, and deviations from planarity of surface may be detected by scanning electron microscopy (Fig. 8a) and optical interference anisotropy. Transmission electron microscopy shows that dislocations generated during the indentation are confined to a small volume of material (comparable with the width of the disturbed surface) and, therefore, occur in extremely high density for Nb_6C_5 (Figs. 8b and 9). Electron diffraction shows that severe crystal rotations occur within this volume. Multiple patterns of diffuse diffraction spots have been observed which correspond to rotations

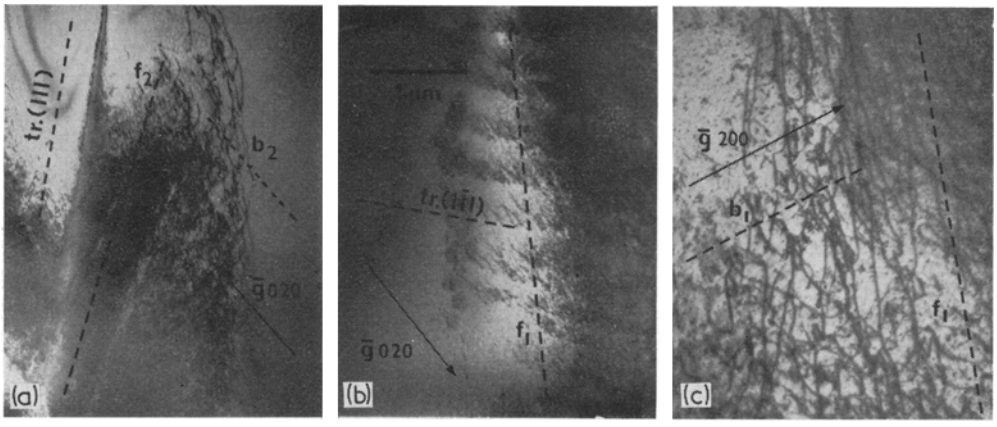

Figure 9 Transmission electron micrographs showing dislocation arrangements round an indentation in [1$\bar{1}$0] orientation on a (001) surface. The projections of the different Burgers vectors for the visible dislocations are indicated for comparison with Fig. 10. (c) is recorded from an annealed crystal and shows the projection of the Burgers vector b_1 corresponding to adjacent facet orientation f_1. The trace of the intersection of indenter facets with the (001) face is shown by the broken line on each micrograph.

from the (100) surface orientation mainly towards (111) with reverse sense of rotation on either side of indenter. Maximum rotations of 15° to 20° have been recorded after indentation with a ⟨110⟩ Knoop diamond orientation.

Dislocations within the volume of severe crystals rotation occur in such high densities that individual dislocations are visible only at the periphery of the deformed region (Fig. 9). A precise analysis of dislocation Burger's vectors and glide planes is inhibited by the absence of well-defined diffracting conditions in regions of severe lattice rotation. However, most of the dislocations which are visible at the periphery of the deformed region are nearly parallel to ⟨110⟩ and have projected lengths consistent with their lying on {111} planes. These dislocations, together with those in crystals which have been briefly annealed at 1000°C (to reduce the dislocation density; Fig. 9c), have Burgers vectors corresponding to {111} ⟨1$\bar{1}$0⟩ systems with the greatest value of τ_e for an adjacent facet orientation; e.g. for facet f_1 in Fig. 10 most dislocations have Burgers vectors $\boldsymbol{b}_1 = a/2 \mid \bar{1}01 \mid$ on a (111) plane.

Additional short segments of resolvable dislocations with a different slip geometry are frequently observed under diffracting conditions which cause invisibility of most of the high density primary dislocations (Fig. 9b). Their projected length and trace direction indicates a slip plane which is either (1$\bar{1}$1) or (1$\bar{1}\bar{1}$) and

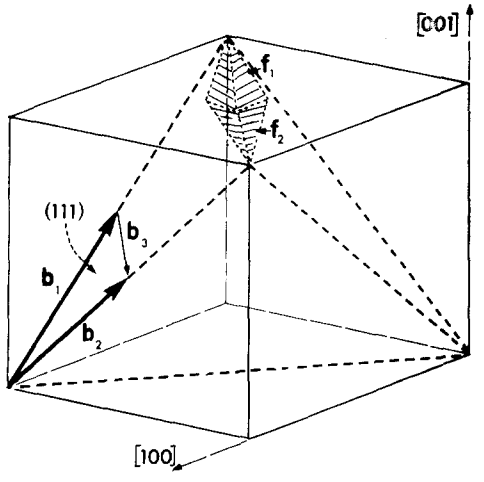

Figure 10 Diagram showing the relation between Knoop indenter orientation and the preferred slip plane (111) containing Burgers vectors $\boldsymbol{b}_1$ and $\boldsymbol{b}_2$ associated with systems of maximum τ_e' for the indenter facets f_1 and f_2.

Burgers vectors of the type $\boldsymbol{b}_1$ or $\boldsymbol{b}_2$, inclined to the (001) surface but usually different from the primary Burgers vector for the adjacent facet. These "supplementary" slip processes may be associated with misalignment of the individual indenter facets from the ⟨110⟩ direction in the indented surface, i.e. they are necessary to accommodate the general crystal shape change imposed by the indenter.

These direct observations of the indented

region by transmission electron microscopy support the analysis of deformation mechanism obtained from hardness anisotropy. They also identify some of the problems in interpretation of such observations for hard materials where the deformed volume is small and severe lattice rotations occur within this volume.

Acknowledgements

We wish to thank W. Precht (of RIAS, Baltimore, Maryland, USA) for supplying the crystal used in this research and H. Mykura for obtaining optical interference micrographs. Technical assistance from G. Smith and I. D. Ward during this project is gratefully acknowledged.

The above paper is based on the final year project of G. Morgan as part of the joint B.Sc. degree in Physics with Materials Science at Warwick University.

References

1. C. A. BROOKES, J. B. O'NIELL and B. A. W. REDFERN, *Proc. Roy. Soc.* (*London*) **A322** (1971) 73.
2. D. J. ROWCLIFFE and G. E. HOLLOX, *J. Mater. Sci.* **6** (1971) 1261.
3. *Idem, ibid* **6** (1971) 1270.
4. W. S. WILLIAMS, Report AFML-TDR-64-25, Part II (1965).
5. D. J. ROWCLIFFE and W. J. WARREN, *J. Mater. Sci.* **5** (1970) 345.
6. C. H. DE NOVION, R. LORENZELLI and P. COSTA, *Compt. Rend. Acad. Sci.* (*Paris*) **263** (1966) 775.
7. J. D. VENABLES, D. KAHN and R. G. LYE, *Phil. Mag.* **18** (1968) 177.
8. M. H. LEWIS, J. BILLINGHAM and P. S. BELL, "Electron Microscopy and Structure of Materials" (University of California Press, Berkeley, 1972) p. 1084.
9. J. BILLINGHAM, P. S. BELL and M. H. LEWIS, *Phil. Mag.* **25** (1972) 661.
10. J. D. VENABLES and M. H. MEYERHOFF, Proc. NBS Symposium on Novel High Temperature Materials (1972).
11. R. H. J. HANNINK, D. L. KOHLSTEDT and M. J. MURRAY, *Proc. Roy. Soc.* (*London*) **A326** (1972) 409.
12. J. BILLINGHAM, P. S. BELL and M. H. LEWIS, *Acta Cryst.* **A 28** (1972) 602.
13. M. SAUVAGE and E. PARTHE, *ibid* **A28** (1972) 607.
14. F. W. DANIELS and C. G. DUNN, *Trans. ASM* **41** (1949) 419.
15. G. E. HOLLOX, *Mater. Sci. Eng.* **3** (1968/69) 21.
16. R. G. LYE, Proc. NBS Symposium on Novel High Temperature Materials (1972).
17. R. H. J. HANNINK and M. J. MURRAY, *Acta. Metallurgica* **20** (1972) 123.

Received 10 September and accepted 16 October 1973.